Optimized single-qubit gates for Josephson phase qubits

Shabnam Safaei,[1,*] Simone Montangero,[1,2] Fabio Taddei,[1] and Rosario Fazio[1]
[1]*NEST-CNR-INFM and Scuola Normale Superiore, Piazza dei Cavalieri 7, I-56126 Pisa, Italy*
[2]*Institut für Quanteninformationsverarbeitung, Universität Ulm, D-89069 Ulm, Germany*
(Received 24 November 2008; revised manuscript received 22 January 2009; published 25 February 2009)

In a Josephson phase qubit, the coherent manipulations of the computational states are achieved by modulating an applied ac current, typically in the microwave range. In this work, we show that it is possible to find optimal modulations of the bias current to achieve high-fidelity gates. We apply quantum optimal control theory to determine the form of the pulses and study in details the case of a NOT gate. To test the efficiency of the optimized pulses in an experimental setup, we also address the effect of possible imperfections in the pulses shapes, the role of off-resonance elements in the Hamiltonian, and the effect of capacitive interaction with a second qubit.

DOI: 10.1103/PhysRevB.79.064524 PACS number(s): 85.25.Cp, 03.67.Lx, 02.30.Yy

I. INTRODUCTION

Over the past decades, together with the development of the theory of quantum information[1] there has been an increasing effort to find those physical systems where quantum information processing could be implemented. Among the many different proposals, devices based on superconducting Josephson junctions are promising candidates in the solid-state realm (see the reviews in Refs. 2–5). Josephson qubits can be categorized into three main classes: charge, phase, and flux qubits, depending on which dynamical variable is most well defined and consequently which basis states are used as computational states $|0\rangle$ and $|1\rangle$.

Phase qubits,[6–8] subject of the present investigation, in their simplest configuration can be realized with a single current-biased Josephson junction. For bias lower than the critical current, the two lowest eigenstates of the system form the computational space. The application of a current pulse, with frequency which is in resonance with the transition frequency of the two logical states—typically in the microwave range—allows to perform all desired single bit operations. Recent experiments[9,10] have realized both single-bit and two-bit gates in capacitive-coupled phase qubits. In the experiments conducted so far, motivated by similar approach in NMR, the amplitude of the microwave current used to perform the qubit manipulation has a Gaussian shape.[9,11] It turns out that Gaussian pulses perform better when their duration time is longer.[11] However, even for long pulses, the error of NOT gate is always higher than 10^{-3}. The importance of achieving fast quantum gates with high fidelity raises the question whether there are modulations other than Gaussian, which lead to high fidelities even when the duration time of the pulse is short. Some theoretical work has already been done in this direction to examine the efficiency of different modulations.[11,12] In the present paper, we follow a different approach as compared to Refs. 11 and 12 and show that by employing the quantum optimal control theory,[13–16] we can further improve the (theoretical) bounds on the error of gate operations.

Quantum optimal control has been already applied to optimize quantum manipulation of Josephson nanocircuits in the charge limit.[17–20] Here we want to test this method in the opposite regime of phase qubit[21] and see whether it is possible to find optimal modulations of microwave pulses, with different duration times, which give very good fidelity for single bit operations.

The paper is organized as follows. In Sec. II we will describe the model for the phase qubit and the Hamiltonian used in the rest of the paper. In Sec. III we present the NOT quantum gate which we have chosen to optimize. Then a brief introduction to the quantum optimal control algorithm which is used for this work will be given in Sec. IV. The numerical results for a phase qubit will be presented in Sec. V. The achieved accuracy for desired operation discussed in Sec. V A is further tested against possible imperfections in the pulses shape (Sec. V B), the presence of off-resonance elements in the Hamiltonian (Sec. V C), and the possible presence of the interqubit capacitive interaction in multiqubit systems (Sec. V D). The specific question of the leakage out of the Hilbert space is addressed in Sec. VI, where we provide numerical results obtained for a junction with five levels inside its potential. A summary of the results obtained and possible perspectives of this work will be presented in the concluding remarks in Sec. VII.

II. SINGLE-JUNCTION PHASE QUBIT

A phase qubit can be realized by a flux-biased rf superconducting quantum interference device (SQUID),[22] a low inductance dc SQUID,[8] or a large inductance dc SQUID.[6] In its simplest design, a phase qubit consists of a single Josephson junction [Fig. 1(a)] with critical current I_0 and a biasing dc current I_{dc}. The Hamiltonian has the form

$$H_{\mathrm{dc}} = -E_C \frac{\partial^2}{\partial \delta^2} - E_J \cos(\delta) - \frac{I_{\mathrm{dc}}\Phi_0}{2\pi}\delta, \tag{1}$$

where $E_C=(2e)^2/2C$ and $E_J=I_0\Phi_0/2\pi$ are, respectively, the charging energy and the Josephson energy of the junction with capacitance C, $\Phi_0=h/2e$ being the quantum of flux, and δ represents the Josephson phase across the junction. The regime in which the superconducting phase δ is the appropriate quantum variable is reached when $E_J \gg E_C$. The potential energy of the system as a function of δ has the form of

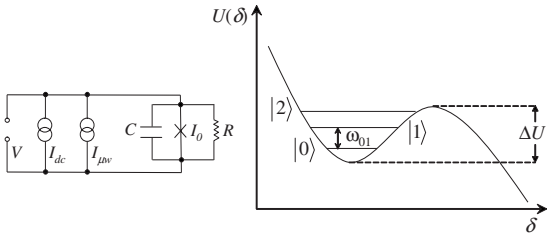

FIG. 1. (a) Schematic drawing of a single-junction phase qubit with capacitance C, resistance R, and critical current I_0 which is biased by a dc current $I_{\rm dc}$. A microwave pulse $I_{\mu w}=I(t)\cos(\omega t+\varphi)$, with frequency $\omega=\omega_{01}$, is applied to make transitions between the two lowest-energy levels of the system $|0\rangle$ and $|1\rangle$. (b) By neglecting the resistive branch, the potential energy of the system U, as a function of the Josephson phase across the junction δ, has the form of a tilted washboard potential. This potential is defined by the height of the well ΔU and the frequency of the classical oscillations in the bottom of the well.

tilted washboard with quantized energy levels inside each well [Fig. 1(b)]. When $I_{\rm dc}\lesssim I_0$ there are few levels inside each well and the two lowest states $|0\rangle$ and $|1\rangle$, with energies E_0 and E_1 and transition frequency $\omega_{01}=(E_1-E_0)/\hbar \approx 5$ GHz, can be used as computational states. The transition between the two lowest states is made by the use of a microwave current $I_{\mu w}$ of frequency ω which is in resonance with the transition frequency ω_{01}. Transition to higher states $(|2\rangle,|3\rangle\ldots)$, which are out of qubit manifold, are off resonance due to the anharmonicity of the potential well.

To be effectively used as a two-level quantum system, the junction is biased with a dc current slightly smaller than the critical current $I_{\rm dc}\lesssim I_0$. In this regime, the potential energy of the system can be approximated by a cubic potential and the Hamiltonian (1) becomes

$$H_{\rm dc}\approx -E_C\frac{\partial^2}{\partial\delta^2}-\frac{\Phi_0}{2\pi}(I_0-I_{\rm dc})\left(\delta-\frac{\pi}{2}\right)-\frac{I_0\Phi_0}{12\pi}\left(\delta-\frac{\pi}{2}\right)^3. \tag{2}$$

The application of a microwave current $I_{\mu w}=I(t)\cos(\omega t+\varphi)$ is taken into account by adding the linear term $H_{\mu w}=\frac{\Phi_0}{2\pi}I_{\mu w}\delta$ to the Hamiltonian (1). Since the eigenstates of the junction biased with a dc current are used as computational states, it is appropriate to write the full Hamiltonian in the basis of the eigenstates $|n\rangle$ of the system with dc bias current. To examine the effect of microwave current, one needs to know the elements of the superconducting phase δ in this basis.

Moving to the rotating frame, which is described by the unitary operator

$$V=\begin{pmatrix}1&0&0\\0&e^{i\omega t}&0\\0&0&e^{2i\omega t}\end{pmatrix}, \tag{3}$$

the Hamiltonian $\tilde{H}$ in the rotating frame is related to the Hamiltonian in laboratory frame H via

$$\tilde{H}=VHV^\dagger-i\hbar V\frac{\partial}{\partial t}V^\dagger, \tag{4}$$

whereas the state of the system in the rotating frame is $|\tilde{\psi}\rangle=V|\psi\rangle$. By introducing $g(t)=I(t)\sqrt{\hbar/2C\omega_{01}}$ and $\Delta_{mn}=\frac{1}{2}\sqrt{\hbar\omega_{01}}\langle m|\delta|n\rangle$, and considering only the first three levels in the well, the Hamiltonian of the phase qubit in the rotating frame takes the following form:

$$\tilde{H}\approx\begin{pmatrix}0&g(t)\Delta_{01}e^{i\varphi}&0\\g(t)\Delta_{10}e^{-i\varphi}&0&g(t)\Delta_{12}e^{i\varphi}\\0&g(t)\Delta_{21}e^{-i\varphi}&-\hbar\delta\omega\end{pmatrix}. \tag{5}$$

Here we have set $E_0=0, \omega=\omega_{01}$ and $\delta\omega\equiv\omega_{01}-\omega_{12}$ and we have assumed that off-resonance terms have negligible effect. As we shall see by a proper choice of φ and microwave current modulation $g(t)$, it is possible to perform single-bit operations on the computational states $|0\rangle$ and $|1\rangle$.

III. NOT GATE

As one can see from the 2×2 top-left block of the Hamiltonian (5), the initial phase of the microwave pulse φ defines the axis of rotation in xy plane of the Bloch sphere for a given state, while the pulse amplitude and duration time define the angle of rotation. For example, by setting $\varphi=0$ $(\varphi=\pi/2)$, such block is proportional to the Pauli matrix σ_x (σ_y), i.e., a rotation around the $x(y)$ axis. In a recent experiment,[10] a π rotation around x has been implemented as a part of a sequence of operations to create entanglement between two phase qubits. This motivates us to set $\varphi=0$ and focus this work on the single-qubit NOT-gate operation consisting of a π rotation around the x axis.

In the typical experiment, a shaped pulse with the following Gaussian modulation:[11]

$$g(t)=\frac{a}{t_g}e^{-(t-\alpha t_g)^2/2t_g^2} \tag{6}$$

is used to induce flips between states $|0\rangle$ and $|1\rangle$ and vice versa. Here a, t_g, and $T=2\alpha t_g$ are, respectively, the amplitude, characteristic width, and total width of the pulse; α being the cutoff of the pulse in time. The actual result of the operation can be quantified by the fidelity $|\langle\psi(T)|\psi_{\rm fin}\rangle|^2$, where $|\psi_{\rm fin}\rangle$ is the desired final state and $|\psi(T)\rangle$ is the state achieved at the end of time evolution starting from initial state $|\psi(t=0)\rangle=|\psi_{\rm ini}\rangle$.

For a π rotation and with a typical cut-off value $(3\leq\alpha\leq 5)$, the amplitude $a\approx\sqrt{\pi/2}$ yields a pretty high fidelity of rotation. More precisely, Fig. 2 shows the error $1-|\langle\psi(T)|\psi_{\rm fin}\rangle|^2$ for a NOT-gate operation on an arbitrary superposition $|\psi_{\rm ini}\rangle=b|0\rangle+c|1\rangle$, which would result in the state $|\psi_{\rm fin}\rangle=b|1\rangle+c|0\rangle$, using a Gaussian pulse with cutoff $\alpha=3$, amplitude $a=1.25$, and duration time T. The leakage outside the qubit manifold defined as $|\langle\psi(T)|2\rangle|^2$ is also shown in Fig. 3. It is worthwhile noting that although the leakage, for long enough pulses, can be of the order of 10^{-7}, the error in the NOT-gate operation is always higher than 10^{-3} (see Ref. 23).

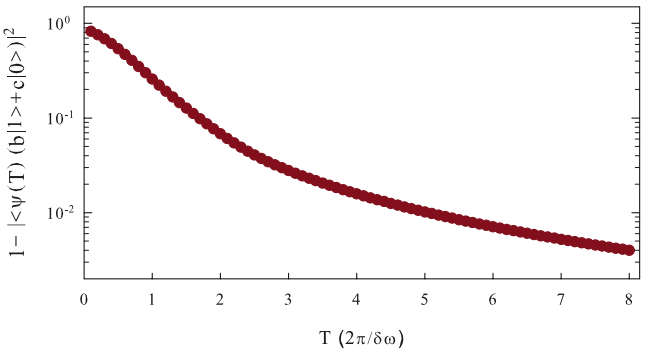

FIG. 2. (Color online) The error of a NOT-gate operation on an arbitrary superposition $b|0\rangle+c|1\rangle$, after applying a Gaussian pulse with amplitude $a=1.25$ and cutoff $\alpha=3$, as a function of the duration time T. $b|1\rangle+c|0\rangle$ is the expected final state and $\psi(T)$ is the final state achieved after applying the Gaussian pulse.

IV. QUANTUM OPTIMAL CONTROL

As we mentioned in Sec. I, in this work we use the quantum optimal control theory in order to obtain microwave current modulations which give rise to a high-fidelity NOT-gate operation for a phase qubit. In this section, we briefly review the optimal control algorithm which we have employed to obtain optimized modulations.

In general, quantum optimal control algorithms[13–15] are designed to lead a quantum system with state $|\psi(t)\rangle$ from an initial state $|\psi(0)\rangle=|\psi_{\text{ini}}\rangle$ to a target final state $|\psi_{\text{fin}}\rangle$ at time T by minimizing a cost functional, which is a measure of inaccuracy of reaching the desired final state. If $|\psi(T)\rangle$ denotes the state achieved at time T, one can consider two different cost functionals:

(i) $e_1 = 1 - |\langle\psi(T)|\psi_{\text{fin}}\rangle|^2$

By minimizing this cost functional, although the population of the desired state $|\psi_{\text{fin}}\rangle$ will be maximized, the overall phase of this state is not forced to be preserved.

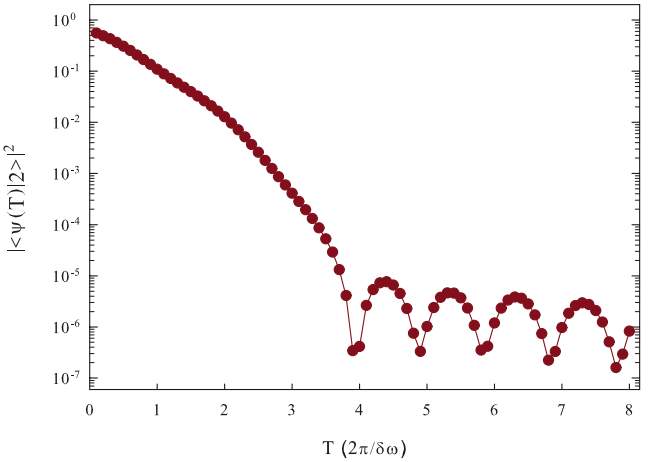

FIG. 3. (Color online) The leakage outside the qubit manifold for a NOT-gate operation on an arbitrary superposition of states $|0\rangle$ and $|1\rangle$, after applying a Gaussian pulse with amplitude $a=1.25$ and cutoff $\alpha=3$, as a function of the duration time T.

(ii) $e_2 = \||\psi(T)\rangle - |\psi_{\text{fin}}\rangle\|^2$

Minimization of this second cost functional, in addition to maximizing the population of the desired state, preserves its overall phase.

In optimal control theory, the minimization of the cost functional is done by updating the Hamiltonian of the system via some control parameters, in an iterative procedure until the desired value of the cost functional is reached. Any specific algorithm which is guaranteed to give improvement at each iteration[24] is called *immediate feedback control* and can be briefly described as follows. Assume that the Hamiltonian of the system depends on a set of parameters $\{u_j(t)\}$ which are controllable. By using a proper initial guess $\{u_j^{(0)}(t)\}$ for control parameters, first the state of the system $|\psi(t)\rangle$ is evolved in time with the initial condition $|\psi(0)\rangle=|\psi_{\text{ini}}\rangle$ giving rise to $|\psi(T)\rangle$ after time T. At this point the iterative algorithm starts, aiming at decreasing the cost functional by adding a correction to control the parameters in each step. In the nth step of this iterative algorithm, (i) an auxiliary state $|\chi(t)\rangle$ is evolved backward in time starting from $|\chi(T)\rangle$ reaching $|\chi(0)\rangle$. In the case of minimizing e_1, $|\chi(T)\rangle = |\psi_{\text{fin}}\rangle\langle\psi_{\text{fin}}|\psi(T)\rangle$ and for minimizing e_2, $|\chi(T)\rangle=2(|\psi(T)\rangle - |\psi_{\text{fin}}\rangle)$. (ii) The states $|\chi(0)\rangle$ and $|\psi(0)\rangle$ are evolved forward in time, respectively, with control parameters $\{u_j^{(n)}(t)\}$ and $\{u_j^{(n+1)}(t)\}$. Here,

$$u_j^{(n+1)}(t) = u_j^{(n)}(t) + \frac{2}{\lambda(t)}\Im\left[\langle\chi(t)|\frac{\partial H}{\partial u_j(t)}|\psi(t)\rangle\right] \tag{7}$$

are updated control parameters. $\lambda(t)$ is a weight function used to fix initial and final conditions on the control parameters in order to avoid major changes at the beginning and at the end of time evolution. These two steps are repeated until the desired value of e_1 or e_2 is obtained.

In order to implement the optimization procedure to a NOT gate for any arbitrary superposition of computational states, one must be able to flip $|0\rangle$ and $|1\rangle$ at the same time (i.e., with same pulse) making sure that the phase relation between them is preserved. This is guaranteed by using the following definition of fidelity:

$$\mathcal{F} \equiv \left|\frac{\langle\psi_0(T)|1\rangle + \langle\psi_1(T)|0\rangle}{2}\right|^2, \tag{8}$$

where $|\psi_0(T)\rangle$ and $|\psi_1(T)\rangle$ are the final states achieved at time T after applying the same pulse on the initial states $|0\rangle$ and $|1\rangle$. The minimization of the cost functional e_1, for flipping at the same time the states $|0\rangle$ and $|1\rangle$, does not necessarily lead to maximization of the fidelity (8) due to possible changes in the phase relation between them. However if e_2 is minimized, the maximal fidelity is also guaranteed. Therefore in order to obtain a high-fidelity NOT gate, it seems more natural to minimize e_2 instead of e_1. However, in the following we will show that although in the ideal case optimized pulses obtained from minimizing e_2 result in much higher fidelity, when more realistic cases are considered optimized pulses from minimizing e_1 lead to higher fidelities, specially for very short pulses. In this work we often use the error $\mathcal{E}=1-\mathcal{F}$ instead of fidelity.

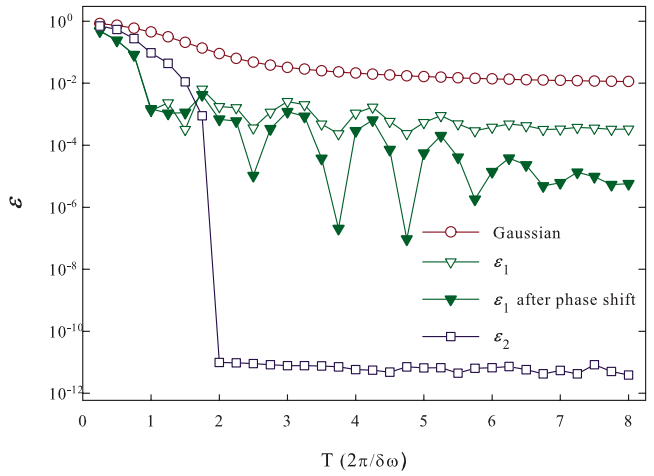

FIG. 4. (Color online) Error for a NOT-gate operation applied to any arbitrary superposition of states $|0\rangle$ and $|1\rangle$ made by pulses with Gaussian modulation (circles) and optimized modulation obtained from minimizing e_1 (unfilled triangles) and e_2 (squares) in a three-level system. Gaussian pulses have amplitude $a=1.25$ and cutoff in time $\alpha=3$. Optimized pulses are obtained after at most 5000 iterations and using Gaussian pulses as initial guess. Filled triangles are obtained by applying a 0.01π phase shift after applying the optimized pulses obtained from minimizing e_1.

V. NUMERICAL RESULTS

In this section, we present the numerical results to show that the quantum optimal control theory allows to optimize the modulation of microwave pulses in order to implement a high-fidelity NOT gate. The optimization is done in the rotating frame and the Hamiltonian (5) is used for the time evolution, while Δ_{ij} are calculated by means of perturbation theory.

A. Optimal NOT gate

By employing the quantum optimal control algorithm described in the Sec. IV and using the modulation of the microwave pulse $g(t)$ as the control parameter, we start from Gaussian pulses (6) of given duration time T as the initial guess and optimize the NOT-gate operation. We will show the results obtained from minimizing both e_1 and e_2 and refer to corresponding errors by $\mathcal{E}_1$ and $\mathcal{E}_2$ and corresponding optimized pulses by g_1 and g_2. The optimization has been stopped when either the cost functionals reached the value 10^{-12} or 5000 iterations are done.

Figure 4 shows the error $\mathcal{E}$ as a function of duration time of the pulse T for the Gaussian pulses used as initial guess (circles) and for the optimized pulses (unfilled triangles and squares). For most of the points, the convergence is reached in much less than 5000 iterations. However for pulses with $T<2\frac{2\pi}{\delta\omega}$, 5000 iterations have been completed. As we expected, minimizing e_2 results in the high-fidelity NOT gate with $\mathcal{E}\approx 10^{-12}$ for all $T\geq 2\frac{2\pi}{\delta\omega}\approx 4$ ns; while for very short pulses it seems that with same number of iterations, minimizing e_1 leads to better results.

In order to understand the reason for the oscillating behavior of $\mathcal{E}_1$ as a function of T, we plot the average value of

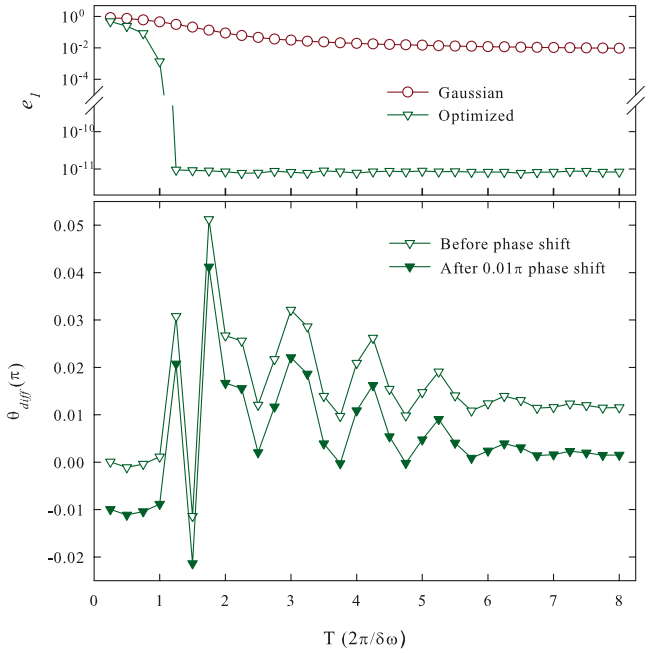

FIG. 5. (Color online) Top panel: the averaged value of e_1 for $|0\rangle\leftrightarrow|1\rangle$ transitions after applying pulses with Gaussian modulation (circles) and optimized modulation (triangles). Optimized pulses are obtained by minimizing e_1. Vertical axis is in logarithmic scale and T is the total width of the pulse. Bottom panel: the phase difference between final $|0\rangle$ and $|1\rangle$ states (after applying the optimized pulses) in units of π. This final phase difference increases the error of NOT-gate $\mathcal{E}_1$ to what has been shown in Fig. 4. In principle, a proper phase-shift gate can compensate this phase difference and decrease the error to 10^{-12}.

e_1 for $|0\rangle\rightarrow|1\rangle$ and $|1\rangle\rightarrow|0\rangle$ transitions at the end of optimization (top panel of Fig. 5) which shows that the final value of e_1 for both of these transitions is of the order of 10^{-12}. As we explained in Sec. IV, e_1 is insensitive to the phase of the final state and it turns out that while a given optimized pulse applied to the initial state $|0\rangle$ leads to the final state $e^{i\theta_0}|1\rangle$ then the same pulse might transform the initial state $|1\rangle$ into $e^{i\theta_1}|0\rangle$, i.e., there is a phase difference between the two final states $\theta_{\text{diff}}\equiv\theta_1-\theta_0$. The bottom panel of Fig. 5 shows this phase difference for optimized pulses with given duration time T which increases the error of NOT-gate $\mathcal{E}_1$ to what has been shown in Fig. 4.

Although this phase difference causes a major increase in the error while working with superpositions, the error $\mathcal{E}_1$ is at least 1 order of magnitude smaller than those from Gaussian pulses (Fig. 4). Moreover the final phase difference between $|0\rangle$ and $|1\rangle$ can be compensated by a following phase-shift gate. In Fig. 4 the results after applying a 0.01π (which is approximately the average of θ_{diff} in time) phase shift are also shown (filled triangles) which demonstrate a significant decrease of $\mathcal{E}_1$.

B. Imperfections in the pulse shapes

In this section we study the Fourier transform of the optimized pulses, in order to see how practically they are realizable in the laboratory and to examine the effect of high-

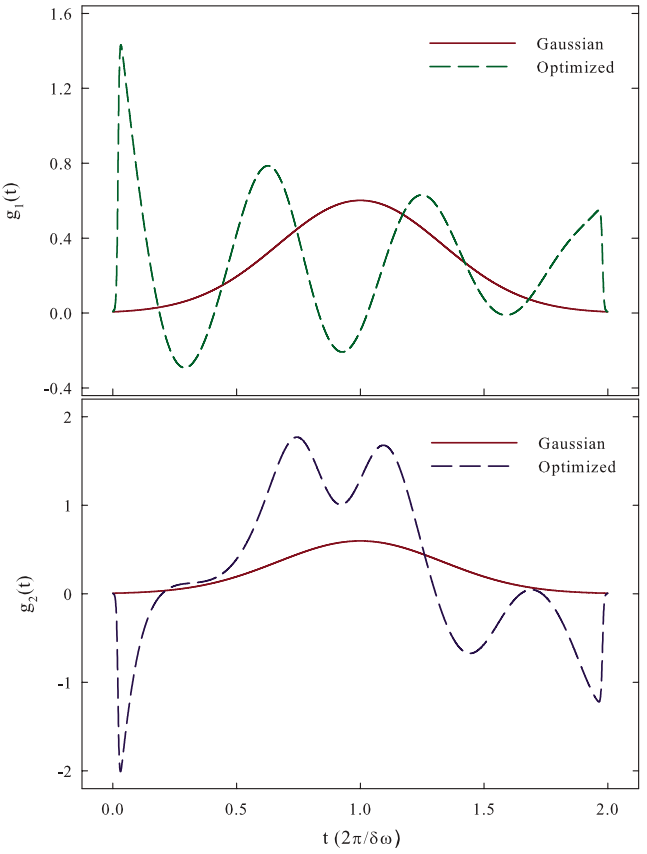

FIG. 6. (Color online) Examples of final optimized modulation of pulses (dashed lines) and the corresponding pulse with Gaussian modulation (solid lines) used as initial guess in optimization process with duration time $T=2\frac{2\pi}{\delta\omega}$ obtained from minimizing e_1 (top panel) and e_2 (bottom panel).

frequency components. Two examples of the final optimized pulses (dashed lines) are shown in Fig. 6: both with the duration time $T=2\frac{2\pi}{\delta\omega}\approx 4$ ns. Optimized g_1 (top panel) and g_2 (bottom panel) are the results of minimizing, respectively, e_1 and e_2. The corresponding Gaussian pulse is also shown in both panels. g_1 is guaranteed to decrease the error of NOT-gate 2 orders of magnitude with respect to the Gaussian pulse, while g_2 would reduce the error up to 10 orders of magnitude.

Figure 7 shows the Fourier transform of the two optimized pulses shown in Fig. 6. To filter out the high-frequency components of the optimized pulses, we set a cutoff frequency ω_{cut} for Fourier components and apply the truncated pulses again and obtain the error. Figure 8 shows the error for a NOT gate for pulses with different duration times as functions of ω_{cut}. $\omega_{01}/2\pi$ is approximately 5 GHz and $\delta\omega$ is typically 10% of ω_{01}. In our calculation $\delta\omega=0.1\omega_{01}$, which means that $\delta\omega/2\pi\approx 500$ MHz.

In the case of $\mathcal{E}_1$, the top panel of Fig. 8 makes it clear that all important harmonics have frequencies smaller than $5\delta\omega$. Note that the number of harmonics included within the cutoff is equal to $T\omega_{\text{cut}}/2\pi$; so that, for $T=N(2\pi/\delta\omega)$, such number is equal to N times the ratio $\omega_{\text{cut}}/\delta\omega$. As a result it seems that for all values of T considered, about 20 harmonics should be sufficient to reach the smallest value of $\mathcal{E}_1$. $\mathcal{E}_2$,

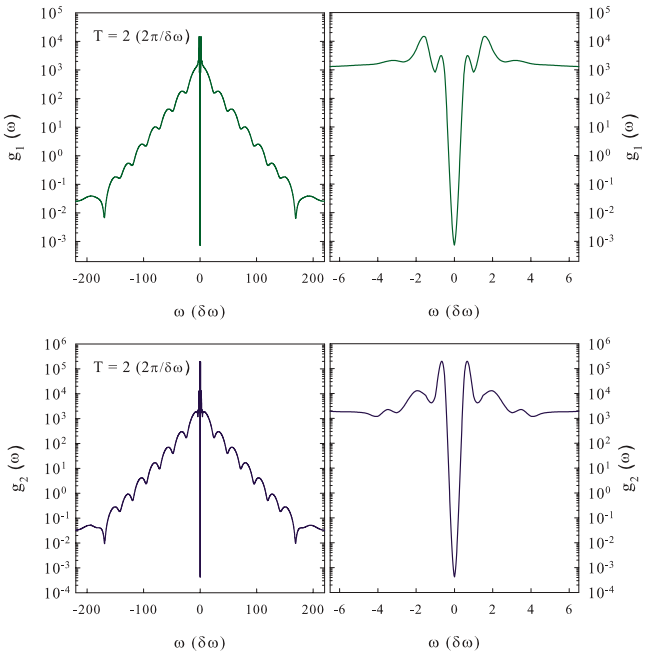

FIG. 7. (Color online) Fourier transform $g(\omega)$ of two optimized pulses shown in Fig. 6 (dashed lines). $g_1(\omega)$ minimizes e_1 and $g_2(\omega)$ minimizes e_2. $\delta\omega$ is chosen to be 10% of ω_{01} and $\omega_{01}/2\pi$ is approximately 5 GHz.

though, seems to be more sensitive to high-frequency components but still about 4 orders of magnitude smaller than $\mathcal{E}_1$ under the cutoff $\omega_{\text{cut}}=10\delta\omega$.

C. Effect of off-resonance terms

As we mentioned previously, we have assumed that off-resonance elements of the Hamiltonian (4) in the rotating frame are negligible and we have used Hamiltonian (5) for calculating the evolution. In this section, we check this assumption by addressing the effect of off-resonance elements by evolving the complete Hamiltonian (4) using the optimized pulses obtained using Hamiltonian (5). Top panel of Fig. 9 shows the error for a NOT-gate operation implemented by Gaussian (circles) and optimized pulses from minimizing e_1 (triangles) and e_2 (squares). For $T>2\frac{2\pi}{\delta\omega}$, the optimized pulses yield a much higher error, with respect to the case when off-resonance terms are neglected, still showing an improvement of 2 orders of magnitude if compared to Gaussian pulses. Bottom panel of Fig. 9 shows the absolute value of the error difference $\delta\mathcal{E}$ obtained by subtracting the error without off-resonance term from the error with off-resonance terms. These figures make it clear that while for Gaussian pulses off-resonance terms can be neglected, for optimized pulses—specially those obtained from minimizing e_2—they are very important. Note that contrary to the ideal case where $\mathcal{E}_2$ was about 8 orders of magnitude smaller than $\mathcal{E}_1$, under the effect of off-resonance terms, $\mathcal{E}_2$ seems to be larger than $\mathcal{E}_1$ specially for very short pulses with $T<2\frac{2\pi}{\delta\omega}$. This means that the assumption of ignoring these terms is more accurate when e_1 is minimized. The simpler shape of the optimized pulses obtained from minimization of e_1 could be a reason for that.

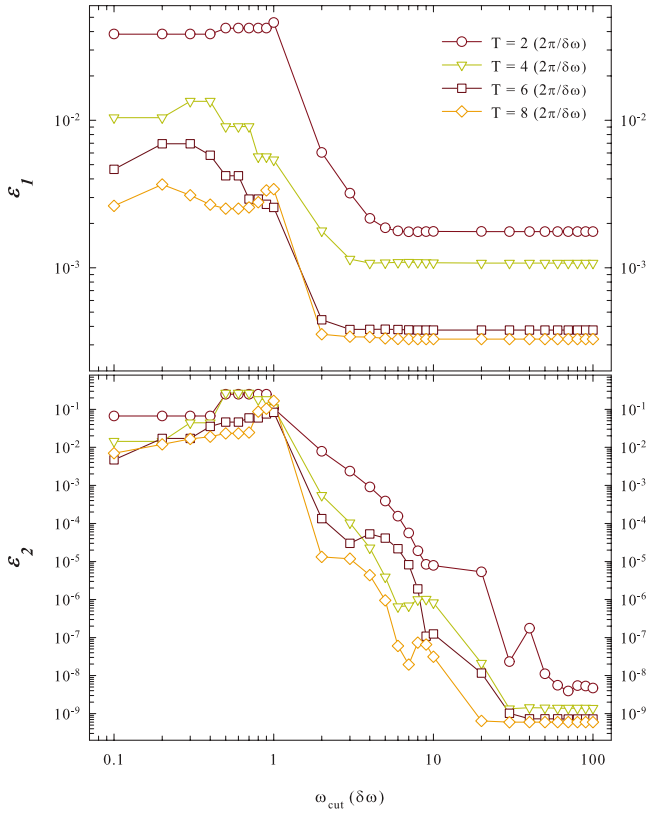

FIG. 8. (Color online) Error $\mathcal{E}$ for a NOT gate with optimized pulses obtained by minimizing e_1 (top panel) and e_2 (bottom panel) as a function of the cutoff frequency ω_{cut}. Integer values of $T\omega_{\text{cut}}/2\pi$ correspond to the number of Fourier components included. $\delta\omega/2\pi$ is approximately 500 MHz.

D. Effect of capacitive interaction

So far we have considered a single qubit with three energy levels and obtained the modulation of the microwave pulses in order to optimize the NOT-gate operation for the two lowest-energy states $|0\rangle$ and $|1\rangle$. It is now interesting to consider the setup[10] containing two qubits interacting via a capacitor. The question that we want to address is what happens if these optimized pulses are applied on the first qubit while the interaction with the second qubit is present.

The interaction Hamiltonian of a circuit with two identical phase qubits has the following form:

$$H_{\text{int}} = -\frac{E_C^2}{E_{C_x}}\left[\left(\frac{\partial^2}{\partial\delta_1^2}+\frac{\partial^2}{\partial\delta_2^2}\right)+2\left(i\frac{\partial}{\partial\delta_1}\otimes i\frac{\partial}{\partial\delta_2}\right)\right], \quad (9)$$

where δ_1 and δ_2 are Josephson phases across junctions 1 and 2 and C_x is the capacitance of the interaction capacitor. Note that the term with second derivative in Eq. (9) can be included in the Hamiltonians of the uncoupled qubits (1) by replacing the charging energy E_C with an effective one $E_{C_{\text{eff}}}=(2e)^2/(2C_{\text{eff}})$, where $C_{\text{eff}}\equiv C^2/C_\Sigma$ and $C_\Sigma=C+C_x$. The Hamiltonian can again be written in the basis of the eigenstates of the uncoupled qubits, and the strength of the interaction Hamiltonian reduces to $(C_x/C_\Sigma)(\hbar\omega_{01})$. We move to the rotating frame described by the unitary operator

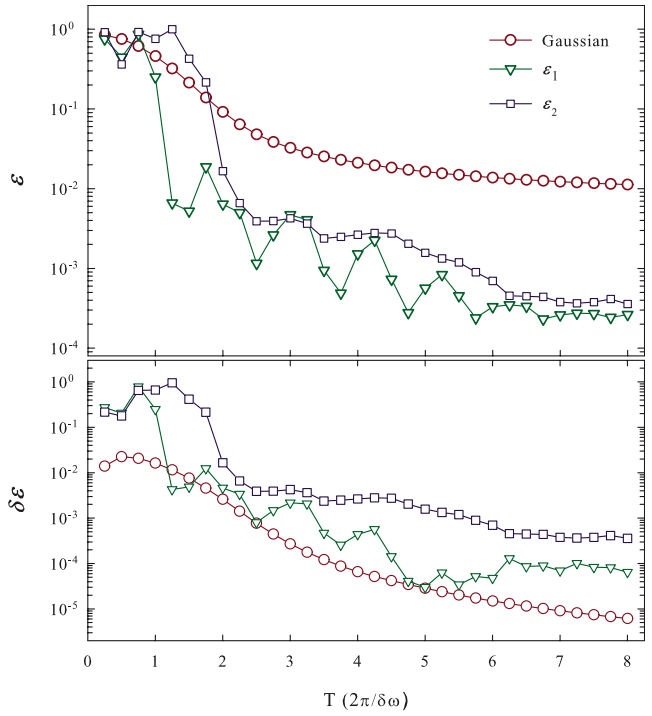

FIG. 9. (Color online) Top panel: the error $\mathcal{E}$ for a NOT gate made by applying microwave pulses with Gaussian modulation (circles) and optimized modulation (triangles and squares) when off-resonance terms are kept. Note that optimized pulses are obtained by excluding off-resonance elements. Bottom panel: the absolute value of error difference $\delta\mathcal{E}$ obtained by subtracting the curves in the top panel from those in Fig. 4. T is the total time width of the pulses.

$$V=\begin{pmatrix}1&0&0\\0&e^{i\omega t}&0\\0&0&e^{2i\omega t}\end{pmatrix}\otimes\begin{pmatrix}1&0&0\\0&e^{i\omega t}&0\\0&0&e^{2i\omega t}\end{pmatrix} \quad (10)$$

and neglect the off-resonance elements of the resulting Hamiltonian. By applying microwave pulse on the first qubit, our aim is to perform a NOT-gate operation on such qubit (namely, $\sigma_{x1}\otimes\mathbb{1}_2$). Since C_x is typically of few femtofarads and C is of the order of picofarad (Refs. 9 and 10), we find $C_x/C_\Sigma\simeq 2.3\times10^{-3}$ which leads to an interaction strength $(C_x/C_\Sigma)\omega_{01}\approx 10$ MHz. Figure 10 shows the error as a function of the time width of the pulse T for both Gaussian (circles) and optimized pulses (triangles and squares). Although the optimized pulses are obtained for a single-qubit system, they still result in smaller error at least for short pulses. These results show the importance of the presence of the capacitive interaction even though the strength of the interaction is small. As it is clear from Fig. 10 for pulses longer than approximately 8 ns ($T=4\frac{2\pi}{\delta\omega}$), the interaction becomes more effective and the error for Gaussian and optimized pulses is very close. Moreover, longer pulses lead to a higher value of error contrary to what happens in the case of a single qubit. In this case also for very short pulses ($T<1.75\frac{2\pi}{\delta\omega}$), $\mathcal{E}_1$ is smaller than $\mathcal{E}_2$ and for $T\geq 2\frac{2\pi}{\delta\omega}$ they are of the same order; although in the ideal case $\mathcal{E}_1$ was 8 orders of magnitude larger than $\mathcal{E}_2$.

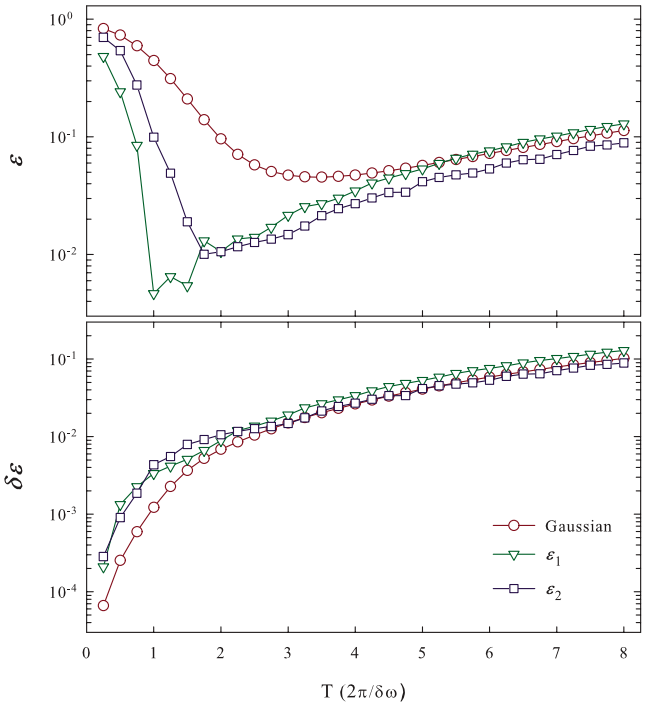

FIG. 10. (Color online) Top panel: error $\mathcal{E}$ for a NOT gate on the first qubit implemented by applying Gaussian (circles) and optimized (triangles and squares) pulses on the first qubit of a two-qubit system in the presence of capacitive interaction. Gaussian pulses have amplitude $a=1.25$ and cutoff in time $\alpha=3$ and are used as initial guess in the optimization procedure. Optimized pulses are obtained from the single-qubit setup. The strength of the interaction is $C_x/C_\Sigma=2.3\times10^{-3}$. Bottom panel: the absolute value of error difference $\delta\mathcal{E}$ obtained by subtracting the curves in the top panel from those in Fig. 4.

The bottom panel of Fig. 10 shows the absolute value of error difference $\delta\mathcal{E}$, which is obtained by subtracting the error of ideal case from the error in the presence of interaction. $\delta\mathcal{E}$ is almost the same in all three cases.

VI. LEAKAGE

As explained in Sec. II, the two lowest-energy levels of a current-biased Josephson junction can be used as $|0\rangle$ and $|1\rangle$ states of a phase qubit. Although it would be desirable to have only two levels inside the potential well of Fig. 1, this is not the case in experimental setups. So far we have included the leakage by considering only an additional third level and showed that it is possible to optimize the pulses in order to gain high fidelity for a NOT gate for a single qubit. In typical experiments, the number of energy levels inside the well varies between three and five. In order to have a more complete understanding of the leakage, in this section we show some results obtained for a five-level system. Since adding more levels to the system decreases the inhomogeneity of the level spacing, we choose $\delta\omega=0.05\omega_{01}$.

Figure 11 shows the error $\mathcal{E}$ for a NOT gate implemented by optimized and Gaussian pulses, which are used as initial guess, for different duration times T. Similar to the case of three-level system, with the same number of iterations, mini-

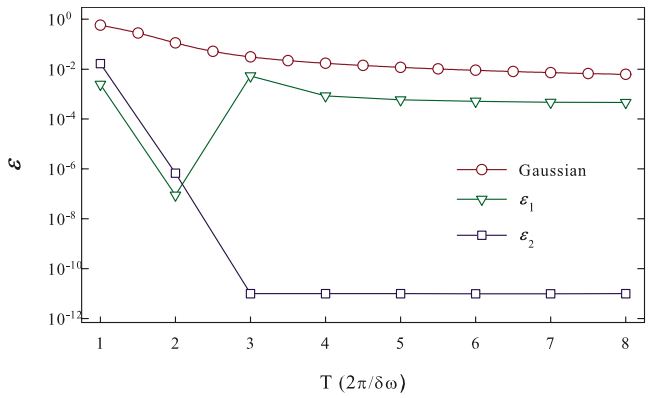

FIG. 11. (Color online) The error $\mathcal{E}$ of NOT gate made by applying Gaussian (circles) and optimized (triangles and squares) pulses as function of duration time of the pulse T. Gaussian pulses have amplitude $a=1.25$ and cutoff in time $\alpha=3$ and are used as initial guess in optimization. Optimized pulses are obtained after at most 15 000 iterations. Physical system contains five energy states and $\delta\omega$ is assumed to be $0.05\omega_{01}$.

mization of e_1 leads to better results for short pulses; while for longer duration times of pulses minimizing e_2 results in the error of NOT-gate $\mathcal{E}_2\approx10^{-12}$. In the case of minimizing e_1, at least 1 order-of-magnitude improvement is achieved for long pulses, although the improvement obtained for pulses with shorter-time width is the best. By looking at the average value of e_1 for transitions between the states $|0\rangle$ and $|1\rangle$ (top panel of Fig. 12) and the final phase difference between them (bottom panel of Fig. 12), one realizes that—as it was observed in three-level system—considerable amount of $\mathcal{E}_1$ is due to the final phase difference θ_{diff}. For instance, the pulse with $T=2\frac{2\pi}{\delta\omega}$ results in a phase difference approximately equal to zero and therefore $\mathcal{E}_1$ for this pulse is of the order of 10^{-8}. A proper phase shift applied after the NOT-gate operation will compensate the phase difference between the final $|0\rangle$ and $|1\rangle$ states and consequently attaining a very high fidelity.

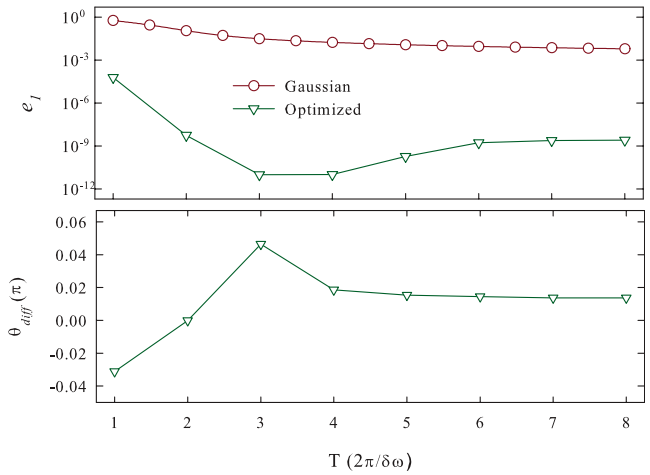

FIG. 12. (Color online) Top panel: the averaged value of e_1 for $|0\rangle\leftrightarrow|1\rangle$ transitions after applying the Gaussian pulses (circles) and optimized pulses (triangles) obtained from minimizing e_1. Vertical axis is in logarithmic scale. Bottom panel: the phase difference between final $|0\rangle$ and $|1\rangle$ states in units of π.

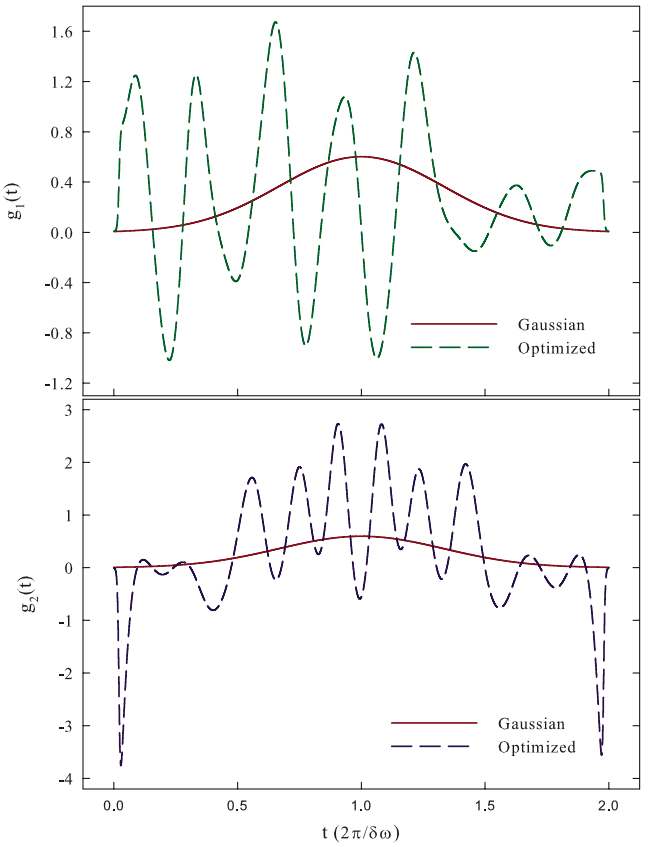

FIG. 13. (Color online) Examples of final optimized modulation of pulses (dashed lines) obtained from minimizing e_1 (top panel) and e_2 (bottom panel) and the corresponding pulse with Gaussian modulation (solid lines) used as initial guess in optimization process with duration time $T=2\frac{2\pi}{\delta\omega}$ in a system with five energy states.

Two examples of pulses with $T=2\frac{2\pi}{\delta\omega}$ are shown in Fig. 13. g_1 is obtained from minimizing e_1 and gives rise to $\mathcal{E}_1 \approx 10^{-8}$, while g_2 is supposed to minimize e_2 with $\mathcal{E}_2 \approx 10^{-7}$. It seems that, compared to three-level system, higher frequencies and amplitudes are needed to reach high fidelity of NOT gate. In three-level system, the iterative optimization algorithm is applied at most 5000 times to reach such fidelities; while with five levels 15000 iterations were needed to obtain the results shown in Figs. 11 and 12. The leakage out of the qubit manifold would be the reason for this.

VII. CONCLUSIONS

In this paper, we have shown that it is possible to optimize single-qubit gates for Josephson phase qubits by employing quantum optimal control theory. We have considered the realistic situation in which, in addition to the two computational basis states $|0\rangle$ and $|1\rangle$, higher-energy states are present, which may lead to leakage. Typically microwave pulses with Gaussian modulation are used to induce transition between states $|0\rangle$ and $|1\rangle$, yielding a quite high fidelity for long pulse durations. For the sake of definiteness, here we have focused on the NOT-gate single-qubit operation and searched for modulations of microwave pulses which optimize such operation, especially for short-duration pulses. The numerical results obtained for a three-level system and neglecting off-resonance terms demonstrate up to 10 orders of magnitude improvement in fidelity of a NOT-gate operation with respect to those obtained through Gaussian modulations. To test the effect of possible imperfections in the pulses shape, we have studied the behavior of the fidelity as a function of the bandwidth of the pulse generator and showed that frequencies not bigger than 2 GHz are needed to gain up to 4 orders of magnitude improvement. Moreover, we have shown that the off-resonance elements of the Hamiltonian, which are usually neglected, can be important for optimized pulses—especially for short pulse duration times—due to the very high fidelity reached. We have also addressed the effect of the presence of a capacitively coupled second qubit and showed that, even though the optimized pulses are obtained for a single qubit, they still lead to a high fidelity for a NOT gate (up to 2 orders of magnitude improvement) especially for very short pulses. Finally, we were able to obtain optimized pulses for a system with five energy levels in which the leakage outside qubit manifold is more severe.

In conclusion, the two-interacting-qubit system deserves for sure further attention. On one hand, in order to improve the fidelity of a single-qubit operation, in the presence of capacitive coupling, it seems that a way to switch the interaction on and off should be found even for optimized pulses of an isolate qubit. On the other hand, obtaining optimized pulses while including the interaction, would be a potential theoretical work to be done.

ACKNOWLEDGMENTS

We would like to acknowledge fruitful discussions with F. W. J. Hekking. We acknowledge support by EC-FET/QIPC (EUROSQIP) and by Centro di Ricerca Matematica "Ennio De Giorgi" of Scuola Normale Superiore. S.M. acknowledges support by EU-project SCALA.

*safaei@sns.it

[1] M. A. Nielsen and I. L. Chuang, *Quantum Computation and Quantum Information* (Cambridge University Press, Cambridge, 2000).

[2] Y. Makhlin, G. Schön, and A. Shnirman, Rev. Mod. Phys. **73**, 357 (2001).

[3] G. Wendin and V. S. Shumeiko, Fiz. Nizk. Temp. **33**, 957 (2007) [Low Temp. Phys. **33**, 724 (2007)].

[4] J. Q. You and F. Nori, Phys. Today **58** (11), 42 (2005).

[5] J. Clarke and F. K. Wilhelm, Nature (London) **453**, 1031 (2008).

[6] J. M. Martinis, S. Nam, J. Aumentado, and C. Urbina, Phys. Rev. Lett. **89**, 117901 (2002).

[7] J. M. Martinis, S. Nam, J. Aumentado, K. M. Lang, and C. Urbina, Phys. Rev. B **67**, 094510 (2003).
[8] J. Claudon, F. Balestro, F. W. J. Hekking, and O. Buisson, Phys. Rev. Lett. **93**, 187003 (2004).
[9] M. Steffen, M. Ansmann, R. McDermott, N. Katz, R. C. Bialczak, E. Lucero, M. Neeley, E. M. Weig, A. N. Cleland, and J. M. Martinis, Phys. Rev. Lett. **97**, 050502 (2006).
[10] M. Steffen, M. Ansmann, R. C. Bialczak, N. Katz, E. Lucero, R. McDermott, M. Neeley, E. M. Weig, A. N. Cleland, and J. M. Martinis, Science **313**, 1423 (2006).
[11] M. Steffen, J. M. Martinis, and I. L. Chuang, Phys. Rev. B **68**, 224518 (2003).
[12] M. H. S. Amin, Low Temp. Phys. **32**, 198 (2006).
[13] A. P. Peirce, M. A. Dahleh, and H. Rabitz, Phys. Rev. A **37**, 4950 (1988).
[14] A. Borzi, G. Stadler, and U. Hohenester, Phys. Rev. A **66**, 053811 (2002).
[15] S. E. Sklarz and D. J. Tannor, Phys. Rev. A **66**, 053619 (2002).
[16] T. Calarco, U. Dorner, P. Julienne, C. Williams, and P. Zoller, Phys. Rev. A **70**, 012306 (2004).
[17] A. Spörl, T. Schulte-Herbrüggen, S. J. Glaser, V. Bergholm, M. J. Storcz, J. Ferber, and F. K. Wilhelm, Phys. Rev. A **75**, 012302 (2007).
[18] S. Montangero, T. Calarco, and R. Fazio, Phys. Rev. Lett. **99**, 170501 (2007).
[19] S. Safaei, S. Montangero, F. Taddei, and R. Fazio, Phys. Rev. B **77**, 144522 (2008).
[20] P. Rebentrost, I. Serban, T. Schulte-Herbrüggen, and F. K. Wilhelm, arXiv:quant-ph/0612165, Phys. Rev. Lett. (to be published, March 2009).
[21] See also P. Rebentrost and F. K. Wilhelm, Phys. Rev. B **79**, 060507(R) (2009); F. Motzoi, J. M. Gambetta, P. Rebentrost, and F. K. Wilhelm, arXiv:0901.0534 (unpublished).
[22] R. W. Simmonds, K. M. Lang, D. A. Hite, S. Nam, D. P. Pappas, and J. M. Martinis, Phys. Rev. Lett. **93**, 077003 (2004).
[23] R. Fazio, G. M. Palma, and J. Siewert, Phys. Rev. Lett. **83**, 5385 (1999).
[24] I. R. Sola, J. Santamaria, and D. J. Tannor, J. Phys. Chem. A **102**, 4301 (1998).